Some Characteristics of Permafrost and Its Distribution in the Gaize Area on the Qinghai—Tibet Plateau, China

Authors: Chen, Ji, Zhao, Lin, Sheng, Yu, Li, Jing, Wu, Xiao-dong, et al.

Source: Arctic, Antarctic, and Alpine Research, 48(2) : 395-409

Published By: Institute of Arctic and Alpine Research (INSTAAR), University of Colorado

URL: https://doi.org/10.1657/AAAR0014-023

Arctic, Antarctic, and Alpine Research, Vol. 48, No. 2, 2016, pp. 395–409
DOI: http://dx.doi.org/10.1657/AAAR0014-023

Some characteristics of permafrost and its distribution in the Gaize area on the Qinghai–Tibet Plateau, China

Ji Chen[1,2,3,*], Lin Zhao[1,4], Yu Sheng[1,2], Jing Li[1,2], Xiao-dong Wu[1,4], Er-ji Du[1,4], Guang-yue Liu[1,4], and Qiang-qiang Pang[1,4]

[1]Cold and Arid Regions Environmental and Engineering Research Institute, Chinese Academy of Sciences, Lanzhou, 730000, China
[2]State Key Laboratory of Frozen Soil Engineering, Lanzhou, 730000, China
[3]Beiluhe Observation and Research Station of Frozen Soil Engineering and Environment, 730000, China
[4]Cryosphere Research Station on the Qinghai-Tibetan Plateau, Chinese Academy of Sciences, Lanzhou, 730000, China
[*]Corresponding author: chenji@lzb.ac.cn

A B S T R A C T

An investigation of permafrost in the Gaize area in the west Qinghai-Tibet Plateau in China was conducted in October and November of 2010 and 2011. It was found that mean annual ground temperature was >–1 °C with a permafrost thickness of <60 m in the widespread alpine steppe below an altitude of 5400 m a.s.l. The active layer thickness was usually deeper than 3 m with a maximum of about 5.7 m. Overall, the ice/water content of the top 15 m of frozen soil was usually <10%. The altitudinal limit of permafrost in the alpine steppe was about 5100, 5000, and 4950 m a.s.l. on south-, east-west–, and north-facing slopes, respectively. A permafrost map was constructed using the ARCGIS platform and topographic information from the TOPO 30 digital elevation model. Statistical analysis of the map revealed that permafrost is primarily distributed in the hilly/mountainous areas of Gaize, covering 51% of the study area. The area of permafrost in this map is considerably less than in the Permafrost Map of the Qinghai-Tibet Plateau drawn in 1996. Further analysis revealed that the large difference between the two maps could be attributed to both errors in the earlier mapping method and permafrost degradation.

Introduction

The Qinghai-Tibet Plateau (QTP; 28°–40°N, 70°–104°E) is located in the south-central part of Asia. It has an average elevation of more than 4000 m a.s.l. and it is often referred to as "the third pole" or the "roof of the world." It exerts considerable influence on the natural environment and human activities within its own and neighboring areas, as well as on global climatic changes (Pan et al., 1995a, 1995b; Pan and Li, 1996; Sun, 1996). The QTP contains the largest mid- to low-latitude permafrost area in the world, which covers an area of about 1.15×10^6 km^2, representing about 70% of total permafrost area in China (Zhou et al., 2000; Ran et al., 2012). Permafrost surveys of the QTP began in the 1960s, mainly along the Qinghai-Tibetan Highway (QTH) corridor (Zhou and Du, 1963; Zhou, 1965). During this period, the Tumen and Muli permafrost stations were established on the south slope of the Tanggula and Qilian Mountains, respectively (Li and Guo, 1980; Zhou et al., 2000). The permafrost was investigated thoroughly and a monitoring network was established in the central and eastern QTP during the planning and construction of many key linear projects and infrastructure developments from 1966 to 2010. These projects included the QTH (Zhao et al., 1998; Wu et al., 2005), Qinghai-Tibetan Railway

(Ma et al., 2006), National Highway 214 (NH 214) (Wang et al., 1991; Li et al., 1998; Wang et al., 1999), National Highway 219 (NH 219) (Li et al., 1998; Zhao et al., 2010), Golmud–Lhasa Oil Pipeline (Zhao et al., 1998), Muli Coal Field (Li, 2009), Reshui Coal Field (Zhou et al., 2000), and West Channel Project of the South-North Water Diversion (Zeng et al., 1996). Up until 2012, >100 permafrost monitoring sites had been established in the central and eastern part of the QTP. The characteristics of permafrost, such as its distribution, thickness, ice/water content, mean annual ground temperature (MAGT), and active layer thickness (ALT), have all been described systematically in previous studies of the QTH, NH 214, and in the Qilian Mountains (Tong et al., 1983; Li and Cheng, 1996; Li et al., 1996; Zhou et al., 2000; Wu et al., 2007a, 2007b, 2009; Wu and Zhang, 2008, 2010; Sheng et al., 2012). Based on the studies in the central and eastern part of QTP in the past, permafrost maps along the QTH and NH 214 have been drawn at different periods (Li and Cheng, 1996; Zhou et al., 2000; Li et al., 2009; Ran et al, 2012; Sheng et al., 2012).

Compared with the central and eastern QTP, permafrost surveys of the western part, such as Gaize area, are scarce. Although electronic sounding methods and pit excavation were widely used to survey the permafrost along NH 219 from Yecheng of Xinjiang Autonomous Region to Ali District of the Xizang Autonomous Region, a drilling survey was only conducted in the Tianshuihai Basin (Li and He, 1990; Li and Li, 1991; He, 1991). These surveys first determined the southern and northern boundaries of the permafrost along NH 219 and monitored the ground temperature in this region. The MAGT is –3.2 °C in Tianshuihai at 4800 m a.s.l., and the base of the permafrost is at about 84 m. To study the degradation of the permafrost and its response to climate warming, a station with comprehensive monitoring scheme (measuring air temperature, air humidity, wind direction and speed, rainfall, solar radiation, soil water content, and ground temperature) was built in the Tianshuihai Basin in 2006 (Yu et al., 2006).

Previous studies on permafrost are limited and insufficient to either determine its characteristics or map its large-scale distribution in the western QTP. In the existing small-scale map of the QTP permafrost, the altitudinal limit of permafrost (ALP) was calculated using fitting equations incorporating the MAGT, latitude, and altitude derived from observed data series. Although these equations could be extended to the entire plateau using GIS technology and TOPO 30 digital elevation model (Nan et al., 2002), the applicability of the results might be unsatisfactory because the fitting data were acquired mainly along the QTH, NH 214, and in other eastern parts of the QTP (LIGG, 1988; Li et al., 1998; Zhou et al., 2000; Nan et al., 2002; CAREERI, 2006; Ran et al., 2012). The distribution of permafrost is influenced by the aridity index—that is, the lower boundary of permafrost rises with the increase of the aridity index (Cheng, 1984). On the QTP, the aridity index declines from >15 to 1 with increasing rainfall from the northwest toward the southeast (Lin and Wu, 1981). Along a line of latitude, there is a trend for the ALP to rise from the east toward the west, the ALP in the western QTP might be much higher than in the east. Therefore, the area of permafrost in the western QTP could be overestimated using the ALP model based on the eastern part of the QTP.

Recent climatic warming has resulted in rising permafrost temperatures, which have led to an increase of the ALT and a lifting of the ALP on the QTP (Wang et al., 2000; Wu et al., 2005). Permafrost in the western QTP has also experienced degradation over past decades. As a part of the cryosphere, permafrost has an important role in local climate, water resources, and vegetation. The recent increases in geotechnical engineering and other human activities in the western QTP have meant that this role has become even more critical. The aim of this paper is to present the characteristics of permafrost in the Gaize area using borehole, pit, vegetation, ground temperature, and geophysical data obtained by field survey in 2010 and 2011. It is also intended to provide a general reference concerning permafrost degradation since the 1980s based on the analysis of past climatic changes and comparison with the existing map of permafrost within the study area.

Study Area and Field Investigation

Study Area

In 2010 and 2011, an investigation of the permafrost was undertaken in the Gaize area of the west-

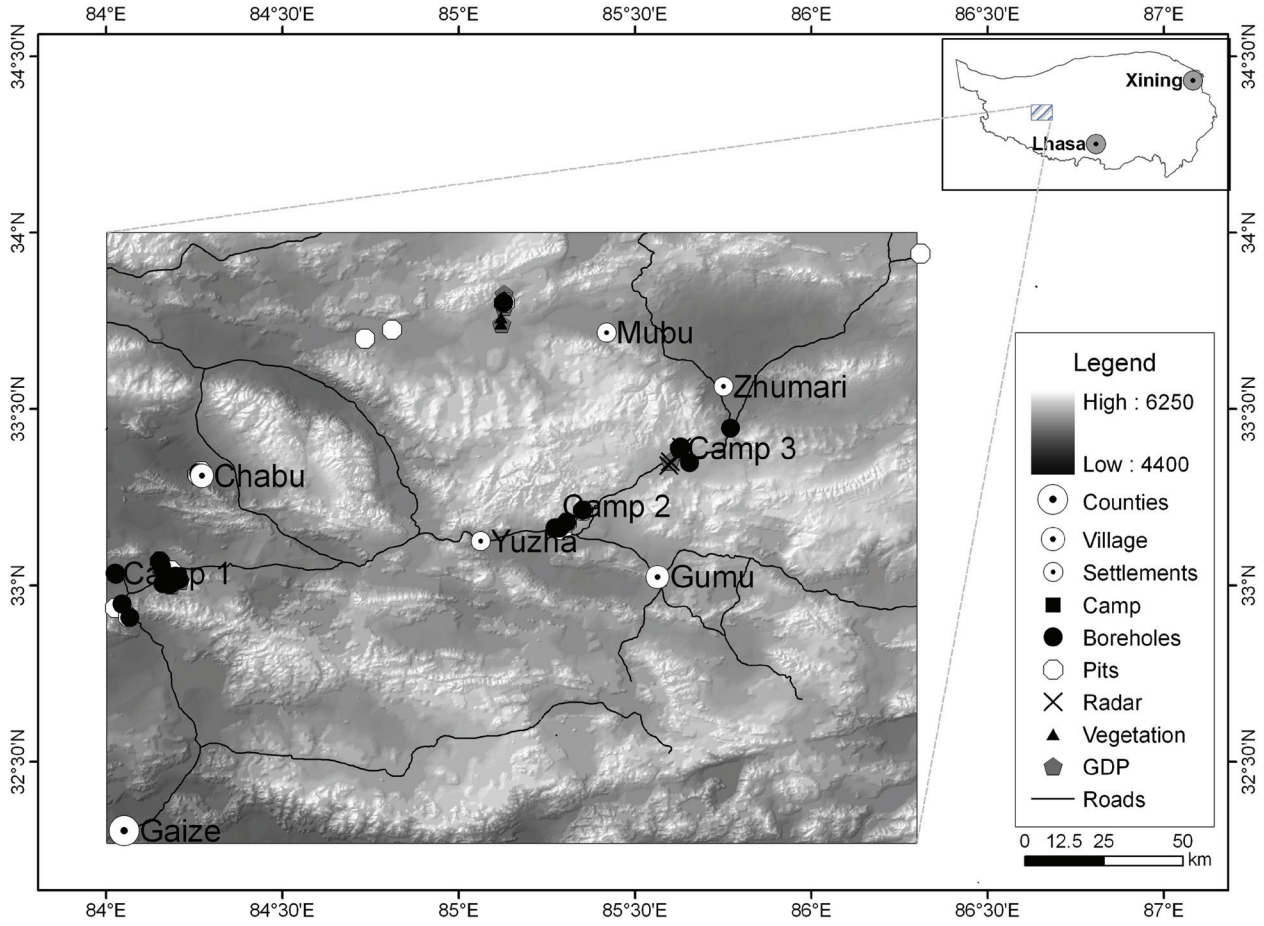

FIGURE 1. Study area of Gaize and its location on the Qinghai–Tibet Plateau.

ern QTP (32°16′–34°00′N, 84° 00′–86°18.5′E; Fig. 1). The region covers an area of 41,256 km^2 and the altitude varies from 4400 to 6200 m a.s.l. The mean annual air temperature (MAAT) of the studied region is higher than that of the eastern QTP at the same latitude and altitude. Data observed at Gaize weather station (4420 m a.s.l.) during the past 30 years indicate that the MAAT is about 0 °C with extreme low of –44 °C recorded in December 1987. The mean annual wind speed is 4.3 m s^{-1} with extreme maximum wind speed at 36.0 m s^{-1}. The average annual precipitation is about 200 mm with a maximum of 296 mm measured in 1977. On average, there are 60 snow days and 3160 sunshine hours annually, and the annual total radiation is 8×10^8 J m^{-2}. The altitude of the investigated area is 0–1800 m higher than Gaize County town, and hence, the MAAT is estimated ranging from –10 °C to 0 °C based on the correlation between MAAT and altitude. According to the previous permafrost map and the relationship between the MAAT and permafrost, the study region is located in the transitional zone from discontinuous permafrost to continuous permafrost (Li and Cheng, 1996).

Dozens of inland rivers are distributed within the region, although they are seasonal rivers and there is no running water in the winter. There are >10 saltwater lakes, among which the largest is about 50 km^2 but most of them are <10 km^2 in size. The land is covered mainly by alpine steppe and alpine meadow. Alpine steppe is the primary vegetation type of the region, for which the vegetation cover is <50%. *Stipa-urpurea griseb* is the dominant species and the edificator of the alpine steppe; the second most prevalent species is *Carex moorcroftii*. The alpine meadow is often small and patchy, and it can be found on the north-facing slope and in wet lowlands. Surface soil horizons formed mainly

in eolian sand and silt can only be found in depressions and around the lakes.

Field Investigation

A substantial amount of field work was conducted during the period from 14 October to 19 November 2010. This included 14 ground-probing radar (GPR) profiles with a total length of 20.7 km, 22 ground data processing (GDP) profiles (executed using a multifunctional electrical workstation) with a total length of 18.4 km, 20 test pits, and 22 boreholes with a total drilling length of 330 m. The average distances between adjacent survey points were 1 and 50 m for the GPR and GDP, respectively. The depths of the test pits varied from 1.0 to 3.9 m. The minimum and maximum depths of the drilled boreholes were 6 and 56 m, respectively; the depth of most boreholes was 15 m. The entire survey site is shown in Figure 1. The locations, land surface conditions, depths, and permafrost states of the boreholes are listed in Table 1. The test pit information is not presented here because permafrost was found in only three pits.

To eliminate thermal disturbance created by the drilling work in 2010 and to measure the MAGT accurately, ground temperatures were measured in October 2011 and in the following years (including 2012–2014). The temperature probes used were produced by the State Key Laboratory of Frozen Soil Engineering. These were fixed within a string of cable and the length of cable depended on the depth of the borehole (ranging from 6 to 60 m). The intervals between the probes were 0.5 m over the

TABLE 1

Locations, land surface conditions, and other relevant information concerning the investigated borehole sites.

No.	Lat. (°N)	Long. (°E)	Alti. (m,a.s.l.)	VC (%)	SA (°)	SG (°)	WC (%)	Depth (m)	ALT (m)	Comments
ZK01	32.94	84.04	4730	20	0	2.5	5.9	8.0	—	NP
ZK02	32.91	84.07	4840	30	0	2.0	7.3	7.7	—	NP
ZK03	33.07	84.15	4740	60	10	5.0	23.0	15.0	2.6	
ZK04	33.07	84.15	4760	20	0	1.0	6.8	7.5	3.5	
ZK05	33.05	84.16	4740	25	180	4.0	6.9	15.0	5.7	
ZK06	33.00	84.16	4800	20	270	2.0	9.5	8.0	—	NP
ZK07	33.00	84.18	4920	10	270	8.0	8.4	8.0	—	NP
ZK08	33.31	84.26	4540	80	0	1.5	12.9	8.0	—	NP
ZK09	33.02	84.21	5010	35	0	7.0	16.2	15.0	3.5	
ZK10	33.03	84.20	4890	20	0	8.0	13.3	8.0	—	NP
ZK11	33.03	84.03	4630	80	210	2.0	10.4	15.0	—	NP
ZK12	33.16	85.29	5020	15	180	15.0	9.1	15.0	—	NP
ZK13	33.18	85.31	5120	15	270	30.0	6.6	15.0	3.8	
ZK14	33.21	85.35	5130	60	200	60.0	12.0	15.0	3.5	
ZK15	33.39	85.63	5130	10	200	4.0	3.2	15.0	6.0	
ZK16	33.39	85.63	5120	80	200	4.0	6.0	15.0	4.5	
ZK17	33.39	85.63	5120	80	200	4.0	21.4	10.3	3.7	
ZK18	33.39	85.36	5120	10	200	4.0	3.5	15.0	3.3	
ZK19	33.35	85.65	5050	5	180	1.0	4.6	12.0	4.0	
ZK20	33.45	85.77	4900	35	70	1.0	9.5	6.0	—	NP
ZK21	33.80	85.13	5020	40	180	1.0	4.5	40.0	3.0	
ZK22	33.39	85.63	5120	40	200	1.0	5.3	56	3.5	

Notes: Lat.—latitude; Long.—longitude; Alti.—Altitude; VC—vegetation cover; SA—slope aspect; SG—slope gradient; WC—water content of top 0.5 m soil layer; ALT—active layer thickness; NP—no permafrost.

first 3 m, and every 1.0 m thereafter. The temperature probes were measured manually using a Fluke 187 multimeter. The accuracy of this method is ±0.05 °C.

Determination of Permafrost, MAGT, and ALT

Permafrost refers to soil/rock that remains at or below 0 °C for at least two consecutive years (Washburn, 1979; French, 2007). In the field, permafrost can be distinguished based on ground temperature and the thermal state of soil water. The ground temperatures in the study area were not monitored consecutively after the borehole was completed in 2010; temperature measurement was only performed once each year from 2010 to 2014. Although the monitoring work was discontinuous, the bottom temperatures of all the boreholes remained largely stable. Compared with the temperatures recorded in 2010, sites with a negative temperature at the bottom of the borehole remained frozen, whereas sites with a positive temperature remained thawed. In fact, the thickness of the active layer is usually <6 m unless bedrock is encountered. Monitoring results along the QTH from 2006–2010 verified that the ALT was not >6 m at 26 sites but <4 m in most sites (Wu et al., 2012). Therefore, negative bottom temperatures can generally be used to determine the existence of permafrost if the borehole is deeper than 6 m.

Physical state of water can be used for the rapid determination of the permafrost in the field. However, reliability of this method is related closely to the depth and morphological features of the ice, salinity, and other properties of the soil, and experience of staff. In this study, to avoid misjudgment, the temperatures of the borehole and the pit were measured. The temperatures of the boreholes were not measured until their thermal states became stable. Unlike boreholes, the temperatures of the pit profiles were only measured once, immediately after the pit was opened. Because pits can be excavated in a relatively short time, the thermal disturbance is very small and the above method can obtain correct temperatures.

The MAGT is generally measured at the depth where the annual fluctuating ground temperature is <0.1 °C. The depth for the MAGT varies from 10 to 15 m on the QTP, depending on the soil/rock properties and annual air temperature amplitude (Qin et al., 2014). The depths of the boreholes in this field investigation were all not within the range. Therefore, to ensure the comparability of ground temperature, the MAGT was measured at the bottom for boreholes with depths <15 m and at the depth of 15 m for boreholes with depths ≥15 m.

ALT refers to the soil layer that experiences annual thawing and freezing (Washburn, 1979). It plays a significant role in the process of mass and energy exchanges between the permafrost and the atmosphere (Cheng and Wu, 2007). Because of its susceptibility to climate change and its significant effect on the hydrology and ecosystem, the ALT has become a topic of considerable interest (Zhang et al., 2005). Because the soil salinity, other soil properties, and water content could alter the freezing point of soil water, it is difficult to determine the ALT precisely by measuring the temperature. Furthermore, the ground temperatures of the boreholes were only measured once a year in this study. It would therefore appear impossible to determine the ALT by use of the maximum penetration of the 0 °C isotherm (Nelson et al., 1998; Brown et al, 2000; Frauenfeld et al., 2004). In high latitude areas, the ALT is often <1 m, which has a relatively large interannual and spatial variation. However, except for the increase due to climate warming, the interannual variation of ALT on the QTP can be regarded as trivial. Based on the statistics of the ALT at 26 sites along the QTH from 2006 to 2010, it was found that the mean interannual variation of the ALT was only 7.8 cm with consideration of climate warming (Wu et al., 2012). The date of the maximum thawing penetration (DMTP) ranges from the end of August to March of the following year (Wu and Zhang, 2010; Qin et al., 2014). The DMTP is related to the ALT, generally occurring in the period from mid-September to mid-October when the ALT is >2.5 m (Lu et al., 2006; Luo et al., 2014). For sites with an ALT ≥4m, the DMTP might be delayed to November or December, or even into the following year. However, the difference between the thawing penetration in October and the maximum thawing penetration is very small and it is often <30 cm (Wu and Zhang, 2010). Additionally, the maximum thawing penetration

might persist for one month or more, because the water content is often very high near the bottom of the active layer (Lu et al., 2006; Luo et al., 2014). The above analysis has indicated that the thawing depth in October could be regarded as the ALT, if the allowable error is 30 cm. Because of the arid climate, interior rivers, and low-lying terrain, soil salinity can be high, especially around the saline lake and in the vast bahadas with saline playa lakes. Salts alter the freezing point of soil water, and consequently the maximum penetration of the 0 °C isotherm does not equate with the ALT. Here, the ALT was determined based on soil/rock properties logged in the boreholes and test pits. According to the profiles of the soil/rock properties completed in October 2010, the upper extreme of the frozen soil and ice was considered the bottom of the active layer. This method is valid if the boreholes and test pits are located in areas that lack talik. In fact, ground temperature measurements in April 2012 and 2013 confirmed there was no talik in the Gaize area, and vertical detachment of frozen soil was not found. Therefore, the above method could be used to determine the ALT within the study region.

Results

MAGT and Permafrost Thickness

The MAGTs of 22 boreholes are illustrated in Figure 2, showing –1 °C < MAGT < 0 °C for 11 sites and MAGT >0 °C for 10 sites. Borehole ZK17 is the only site at which MAGT < –1°C. This borehole is located in a marsh. However, marsh accounts for only 2% of the entire region and hence cannot be considered representative of the Gaize area. Borehole ZK14 is located in alpine steppe. With consideration of the lapse rate of air temperature (i.e., 6 °C 1000 m^{-1}), it can be concluded that the MAGT is <–1 °C at an altitude of about 5400 m a.s.l. and –3 °C at an altitude of about 6000 m a.s.l.

It is well known that permafrost thickness depends on MAGT with an assumption that the geothermic gradient is fixed. Previous studies have suggested that the geothermic gradient varies in the range of 2.5–3.0 °C 100 m^{-1} in the central QTP (Wang et al., 1990). Assuming the geothermal gradient is 2.5 °C 100 m^{-1}, then the permafrost thickness can be estimated at <60 m below 5400 m a.s.l., 60–140 m between 5400–6000 m a.s.l., and >140 m above 6000 m a.s.l. Of the 13 boreholes in permafrost sites, 2 (ZK09 and ZK22) penetrated through the permafrost base. The MAGT for ZK09 is only 0.59 °C, but the borehole logging data confirmed ice-rich permafrost within the range of 3.5–10.0 m. In ZK22, confined water spewed about 0.5 m high at the ground surface when the drilling depth reached 56 m, which indicated that the borehole drilled through the perennial frozen soil layer. According to the soil conditions, the gravelly soil layer at the depth of 55–56 m should be frozen; otherwise, the confined water should erupt at the drilling depth of 55 m because the thawed gravelly soil cannot serve as an aquiclude. One year after the completion of the borehole, the MAGT at the depth of 15 m was found to be –0.14 °C. Boreholes ZK15–18 are located near ZK22. The longest distance between the four boreholes is <200 m and the shortest distance is <50 m. The MAGTs of ZK15–18 range from –1.93 to –0.40 °C. With reference to the permafrost thickness and the MAGTs of neighboring boreholes, the MAGT in ZK22 should be much lower than –0.1 °C. Therefore, it can be concluded that the ground temperature in ZK22 is still unstable 1 year after the completion of the borehole. According to the temperature measurement in October 2011, the ground at depths below 32 m had still not refrozen.

The drilled depth of ZK21 is 40 m, for which the bottom temperature is –0.06 °C (Fig. 3, part a). The ground temperature is –0.38 °C at the depth of 20 m and –0.06 °C at the depth of 40 m; thus, geothermic gradient is 1.6 °C 100 m^{-1}. Based on this value, it can be concluded that the permafrost thickness at this site is about 45 m.

The GDP survey confirmed the above result. Parts b and c in Figure 3 show the changes in the resistivity of soil and its rate of decline with depth, respectively. The absolute value of the rate of decline of resistivity increases continuously with depth varying from 30 to 47 m below the ground surface, while the soil becomes warmer and the ground temperature rises from –0.24 to 0 °C. The resistivity of soil in the frozen state is closely connected to temperature. A rise in temperature results in an increase of the amount of unfrozen water within the soil. With an increase of unfrozen water content, soil resistivity decreases from millions Ω·m to hun-

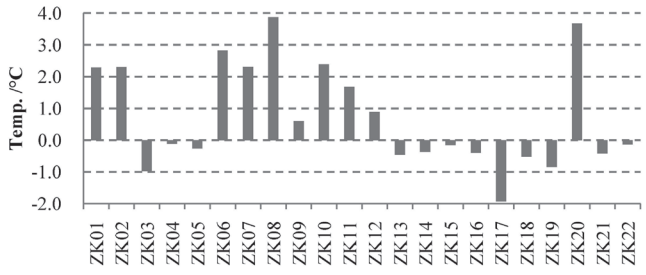

FIGURE 2. Mean annual ground temperature (MAGT) of investigated boreholes. MAGTs were generally measured at the depth of 15 m. For boreholes whose depth is <15 m, bottom temperatures were taken to represent MAGTs.

dreds Ω·m (Cao et al., 2007). At the depth of 47 m, the rate of decline of resistivity begins to decrease with depth, which means that this depth marks an inflection point for resistivity. Geophysical experience shows that an inflection point for resistivity in the permafrost area usually occurs at the permafrost table and base (He, 1991). Therefore, the depth of 47 m can be regarded as the base of permafrost. Temperature measurements and geophysical surveys both indicate that the thickness of the permafrost at ZK21 varies from 45 to 50 m. Borehole ZK21 is located in a swamp, and it is found that permafrost thickness is slightly bigger than the value predicted by the geothermal gradient of 2.5–3.0 °C 100 m^{-1}.

The above analysis verifies that the conclusion regarding permafrost thickness below 5400 m a.s.l. is reasonable and correct. Above 5400 m a.s.l., drilling and geophysical surveys were not implemented because of steep terrain, and therefore verification of the permafrost thickness at such altitude requires further work.

Water/Ice Content of Frozen Soil

Table 1 lists the water content in the 0–0.5 m layer at the 22 drilling sites. Water content is <10% in 15 sites, 10%–20% in 5 sites, and >20% in ZK03 and ZK16. Because of the influence of the arid climate, drought-affected soil is common in the investigated region. Local factors, such as the lowland and surface runoff and the microclimate, lead to more moist soil at ZK03 and ZK16. In soils deeper than 0.5 m, water content changes significantly with depth and location (Fig. 4). As shown in Figure 4, water content is generally <15% both between the depths of 0.5–2.0 m and below 8 m. In the depth interval of 2–8 m, water content for nine boreholes is >20%, and of these, eight have permafrost. Compared with the seasonal frozen area, there is considerable water or ice in the upper permafrost right beneath the active layer, although the investigation area has an arid climate.

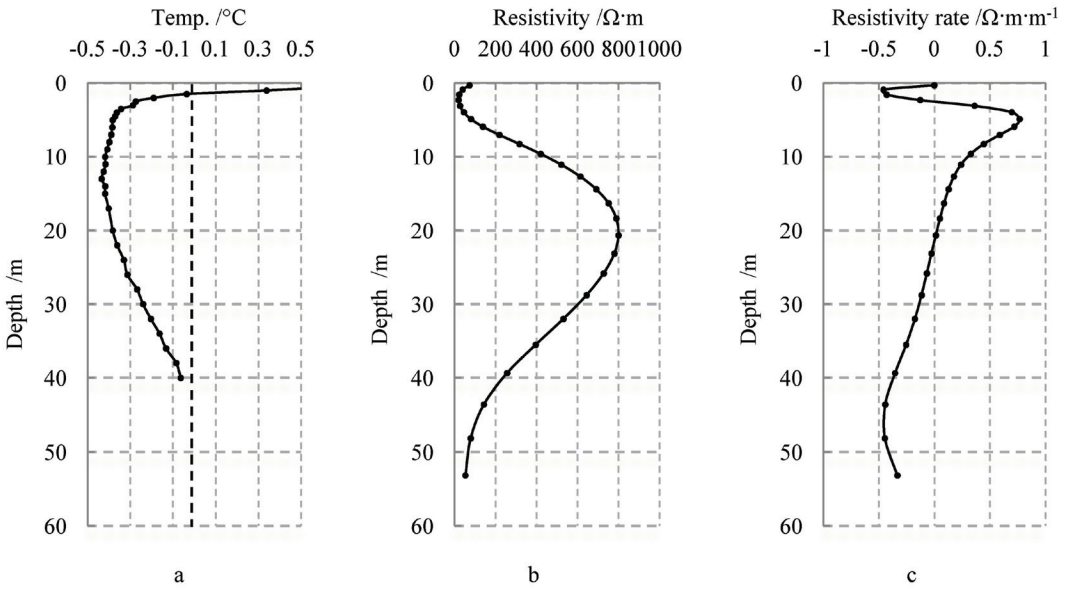

FIGURE 3. Changes of temperature and resistivity with depth at ZK21. (a) Profile of ground temperature, (b) profile of resistivity, and (c) profile of resistivity rate.

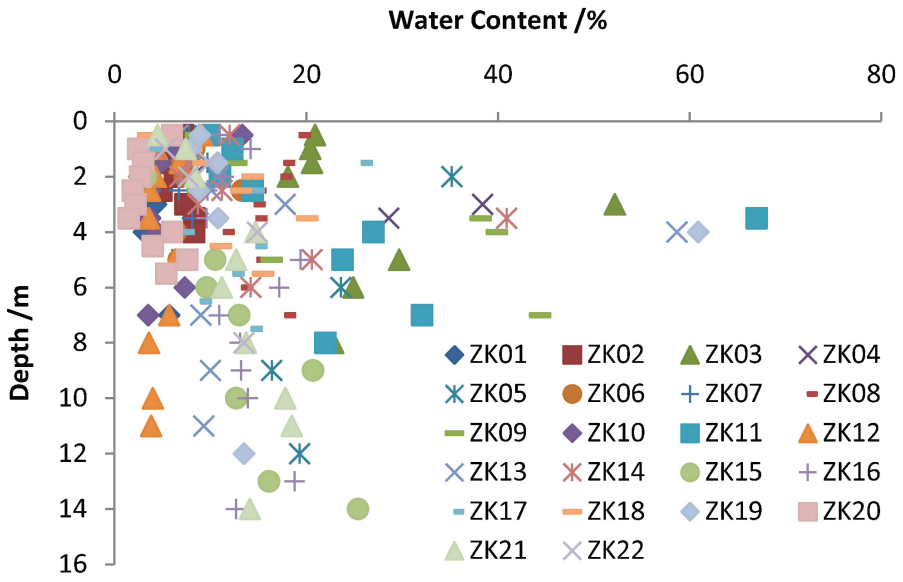

FIGURE 4. Distribution of water content with depth for all the boreholes.

Active Layer Thickness (ALT)

Previous work has suggested that the ALT within the QTP is generally between 2.0 and 2.4 m. An active layer with a thickness of >2.4 m only exists at the top of some mountains (Pang et al., 2009).

Table 1 reveals that among the 13 permafrost sites, the average ALT is 3.9 m, and there is only 1 site (ZK03) with an ALT <3 m. The ALT was determined principally based on the air temperature thawing index in the summer and soil properties, especially the soil water content (Brown et al., 2000; Hinkel and Nelson, 2003; Wu and Zhang, 2010). Because of its large latent heat capacity, soil water content has significant influence on the ALT. Generally, the ALT increases with a decrease of water content. An arid climate with annual rainfall about 200 mm leads to widespread drought-affected soil, and consequently, the ALT is much thicker in the Gaize area than in the east QTP.

Distribution and Mapping of Permafrost

Altitudinal Limit of Permafrost (ALP)

The distribution of permafrost depends on the MAAT that is closely related to the latitude, altitude, and precipitation. In the northern hemisphere, along the same longitudinal axis, the MAAT decreases by about 0.62–0.94 °C for every 1° increase in latitude. The MAAT decreases by <2 °C from 32°N to 34°N on the QTP (Lin and Wu, 1981; Cheng, 1984). Annual precipitation affects the MAAT in the same way in the area south of 40°N, and the QTP is located south of this latitude. The rate of descent of the MAAT with rainfall ranges from 3.8 to 5.4 °C 1000 mm^{-1}. On the QTP, the MAAT will drop by approximately 4 °C if the rainfall increases by 1000 mm (Cheng, 1983; Cheng, 1984). In general, the coverage and type of vegetation act as good indicators of precipitation. For the investigated region that spans 2° of latitude and 3° of longitude (slightly more than 4×10^4 km^2), 81.4% of the area is alpine steppe and 2% marsh. The distribution characteristics of the marsh areas mean that vegetation is affected mainly by landform rather than rainfall. Widespread alpine steppe implies that spatially, the distribution of rainfall is relative even over the Gaize area.

The altitude of this region varies from 4400 to 6200 m a.s.l. It is known that air temperature decreases by 6 °C for every 1000 m rise in altitude. Consequently, the maximal difference in air temperature within the investigated region is about 10 °C. From the perspective of permafrost distribution in this region, altitude is more important than latitude and precipitation. This means that the permafrost distribution could be mapped if the ALP is determined. The contour corresponding to the

MAGT value of 0 °C can be regarded as the ALP. Similar to air temperature, the MAGT also has a linear relationship with altitude. Therefore, the ALP could be calculated using a linear fitting equation for the MAGTs of ZK01, ZK06–ZK16, ZK18, ZK19, ZK21, and ZK22.

Among 22 boreholes, 3 permafrost boreholes (ZK03, ZK04, and ZK05) are located in the same marsh area, which has an altitude of 4800 m a.s.l. The soil in the top 15 m at these sites is composed mainly of wet medium- to fine-textured soils, such as sandy loam and silty clay (Fig. 5). These three boreholes confirmed that the permafrost can develop in areas with altitudes of 4700 to 4800 m, if the slope aspect, water content, and soil physical properties are all favorable (Jin et al., 2008; Lü et al., 2008). However, compared with the alpine steppe, marsh cannot be used to determine the permafrost distribution because of its small proportional representation within the area.

To improve the quality of the statistical analysis, data from some boreholes in the marsh areas were excluded (i.e., ZK03, ZK04, ZK05, and ZK17). Furthermore, boreholes ZK02 and ZK20 were not considered because their base temperature at the depth of 6 m cannot be representative of the MAGT. Figure 6 illustrates the relationship between altitude and MAGT. According to the linear fitting equation, the ALP within the investigated region is 5088 m.

Influence of Slope Aspect on the ALP

The amount of solar radiation received on the ground varies with slope aspect. More solar radiation means higher ground surface temperatures and a higher ALP. The study area is located in the northern hemisphere, which means that south-facing slopes receive more radiation and have higher ground temperatures. Consequently, the ALP is higher on the south-facing slopes than it is on other slopes. For flat ground, it is unnecessary to consider the effects of slope aspect, and therefore its ALP can be regarded as equal to that of east-west–facing

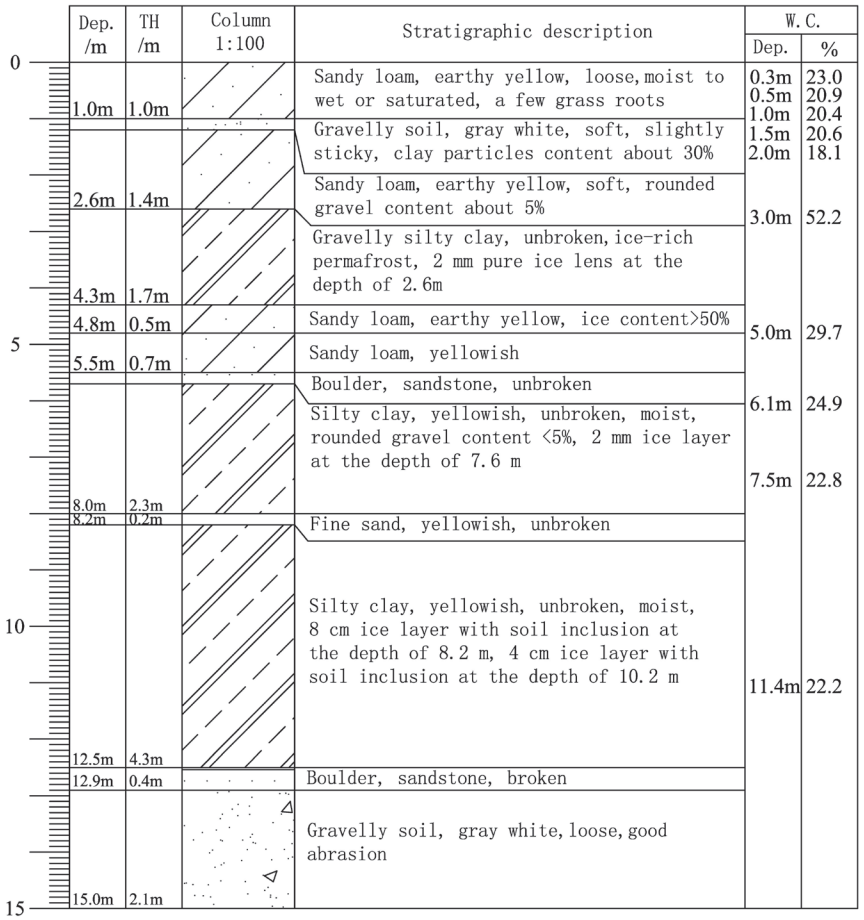

FIGURE 5. Stratigraphic profile of borehole ZK03. Dep. = the depth where the stratum is located, TH = the thickness of the stratum, and W.C. = the soil water content at different depths.

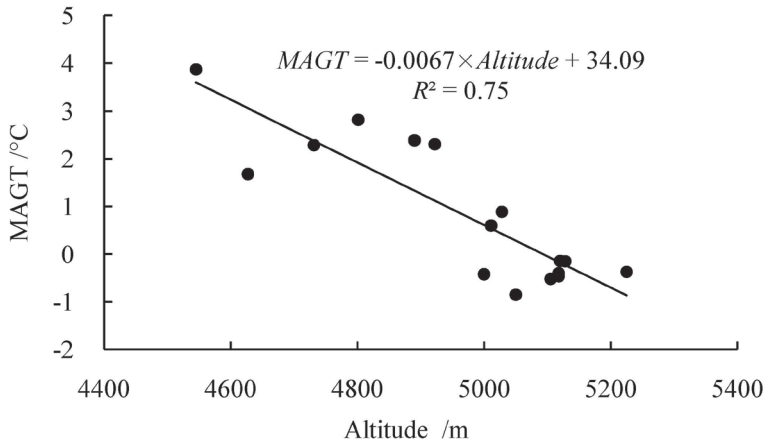

FIGURE 6. Relationship between MAGT and altitude in the investigated area, based on 16 boreholes in alpine steppe.

slope. In the investigated region, terrain fluctuates dramatically and the altitude difference is >1500 m. Therefore, the influence of slope aspect on the ALP must be considered before drawing a permafrost map of this region.

To better understand the distribution of permafrost within this region, only those boreholes within the alpine steppe were analyzed (i.e., ZK01–02, ZK06–10, ZK12–15, ZK20, and ZK22). According to their aspect, these boreholes can be classified into three types: north-facing slopes (ZK01–02 and ZK08–10), south-facing slopes (ZK12, ZK14–15, and ZK22), and east-west–facing slopes (ZK6–7, ZK13, and ZK20). Figure 7 shows the relationship between the ALP and slope aspect. The ALP, calculated using linear fitting, was found to be about 4950 m a.s.l. for north-facing slopes, 5000 m a.s.l. for east-west–facing slopes, and 5100 m a.s.l. for south-facing slopes. As shown in Figure 7, permafrost can exist on north-facing slopes (pink shaded area) below 5000 m a.s.l, and on north-facing and east-west–facing slopes (blue area) at 5000 to 5100 m a.s.l. Furthermore, permafrost can even exist on the south-facing slopes at altitudes >5100 m a.s.l.

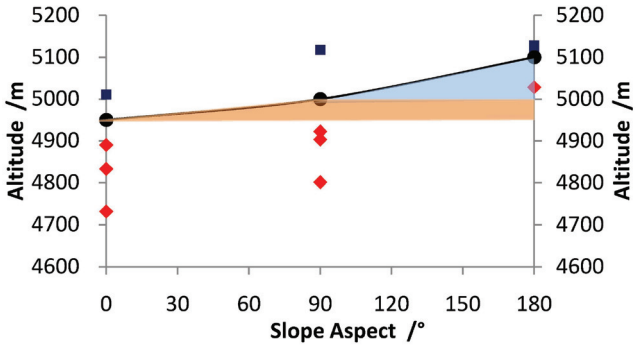

FIGURE 7. Relationship between permafrost and altitude on slopes with different aspects. 0° represents north-facing slopes, 90° represents east-west–facing slopes, and 180° represents south-facing slopes. ZK20 is categorized as being on an east-west–facing slope. The slope aspects of ZK06, ZK07, and ZK13 are given as 90°. Red rhombic dots represent boreholes in the seasonally frozen area, dark blue square dots represent boreholes in the permafrost area, and black round dots represent the altitudinal limit of permafrost on slopes with different slope aspects. Pink shaded area means that there exists permafrost only on north-facing slope, and blue area means that permafrost probably is distributed on the north-facing and east-west–facing slope.

Permafrost Map Based on the Investigation (PMI)

The permafrost map for the investigated region was drawn using ARCGIS version 9. Topographic information for this region was derived from the digital elevation model. The slope aspect and altitude of each grid cell were compared with the ALP. The grid cell was regarded as permafrost if the altitude was higher than the ALP. Finally, the permafrost distribution was mapped using the spatial analysis model of ARCGIS (Fig. 8).

As discussed above, the ALP is 5000 m a.s.l. on flat ground, 4950 m a.s.l. on north-facing slopes, 5000 m a.s.l. on the east-west–facing slopes, and 5100 m

a.s.l. on the south-facing slope. A grid cell was regarded as flat ground if the slope gradient was less than 2°. Under the condition that the slope gradient was more than 2°, slopes were assigned as east, south, west, and north for aspects of 45°–135°, 135°–225°, 225°–315°, 315°–360°/0°–45°, respectively.

According to the map of permafrost distribution within the study region (Fig. 8), the extent of the seasonally frozen ground is 20,929 km^2 (50.7% of the total area), and that of the permafrost is 20,327 km^2 (49.3% of the total area). Additionally, supposing that marshes (2% of the total area) are fully dominated by permafrost, the final proportion of permafrost would be about 51%. In accordance with the classification scheme of spatial continuity, the investigated region is located within a discontinuous permafrost zone (Brown et al., 1997; French, 2007), and the permafrost is distributed in the hilly and mountainous areas. In addition, the seasonally frozen ground is distributed in the bahadas.

Discussion

Prior to 2010, a comprehensive and systematic permafrost investigation in the western QTP had not been conducted because of limited access due to severe climate conditions coupled with high altitudes. Consequently, there is little information regarding the permafrost within this region, with the exception of the Permafrost Map of the Qinghai-Tibet Plateau (Li and Cheng, 1996) and several boreholes along NH 219 in the western QTP (Li and He, 1990; He, 1991; Li et al., 1998). The permafrost coverage around the Gaize area was estimated 91.5% based on the map of Li and Cheng (1996) (Fig. 9).

However, based on the estimation from the current study, only 51% of the Gaize area has permafrost and the ALP increased from about 4650 to about 5000 m a.s.l. The current study found that the warming rate of the MAAT in Gaize County town was 0.44 °C 10 a^{-1} for the period 1971–2007, 0.04 °C 10 a^{-1} for the period 1971–1990, and 0.87 °C 10 a^{-1} for the period 1991–2007 (Tan et al., 2010). It is estimated that the MAAT has increased by about 1.8 °C for the period of 1980–2010. Statistical analysis of soil and air temperatures showed that 50 cm soil temperature has also increased by about 1.8 °C in Gaize County town (Feng and Cai, 2004). Previous studies have found that the rate of ground temperature decrease with altitude fluctuates at around 0.8 °C 100 m^{-1} (Feng and Cai, 2004; Li et al., 2011, 2012; Niu et al., 2013). According to 50 cm soil temperature rise and the regularities of ground temperature with altitude, it can be established that the ALP in the Gaize area has increased on average by 225 m during the period of 1980–2010 and that it is now at 4875 m a.s.l. In fact, the degradation of permafrost lags behind the increase of air and soil temperature. Numerical simulation suggests that the MAGT rises from –1.4 to –0.3 °C over a hundred-year period under the condition of air temperature warming at a rate of 0.04 °C a^{-1} (Wei et al., 1999). The increment of change in the MAGT is much less than in the MAAT. Taking Chumaer station on the QTH as an example, the ground temperature at 20 m depth was stable from 1970 to 1990, whereas the air temperature increased by 0.4 °C (Wang et al., 1996). According to data from eastern QTP, the ALP increased by 40 to 80 m from 1970 to 1996, and the area of permafrost has reduced by 7.1% (Wang, 1997). A later investigation has verified that the ALP in Xidatan rose by 25 m from 1975 to 2005 (Wu et al., 2005). Although the MAAT has risen 1.8 °C, the increment of the ALP within the investigated region is estimated to be 50 to 100 m, and the reduction in permafrost area is estimated at about 10%.

The preceding discussions reveal that the large differences between the two maps could result from errors in the mapping method used to create the map of Li and Cheng (1996). Because of the lack of data regarding the permafrost within this region, a permafrost map was drawn using a Gaussian Model proposed by Cheng (1984). This model does not involve the influence of the aridity index. However, the ALP increases with the aridity index in areas south of 40°N (Cheng, 1984). From the east to the west of the QTP, the aridity index increases from 1.5 to 5 (Lin and Wu, 1981). Consequently, the ALP within the investigated region is 100–300 m higher than in the east, and the area of permafrost is considerably less than shown by the map of Li and Cheng (1996).

Conclusions

Based on data from an investigation of permafrost in 2010, the characteristics of the permafrost

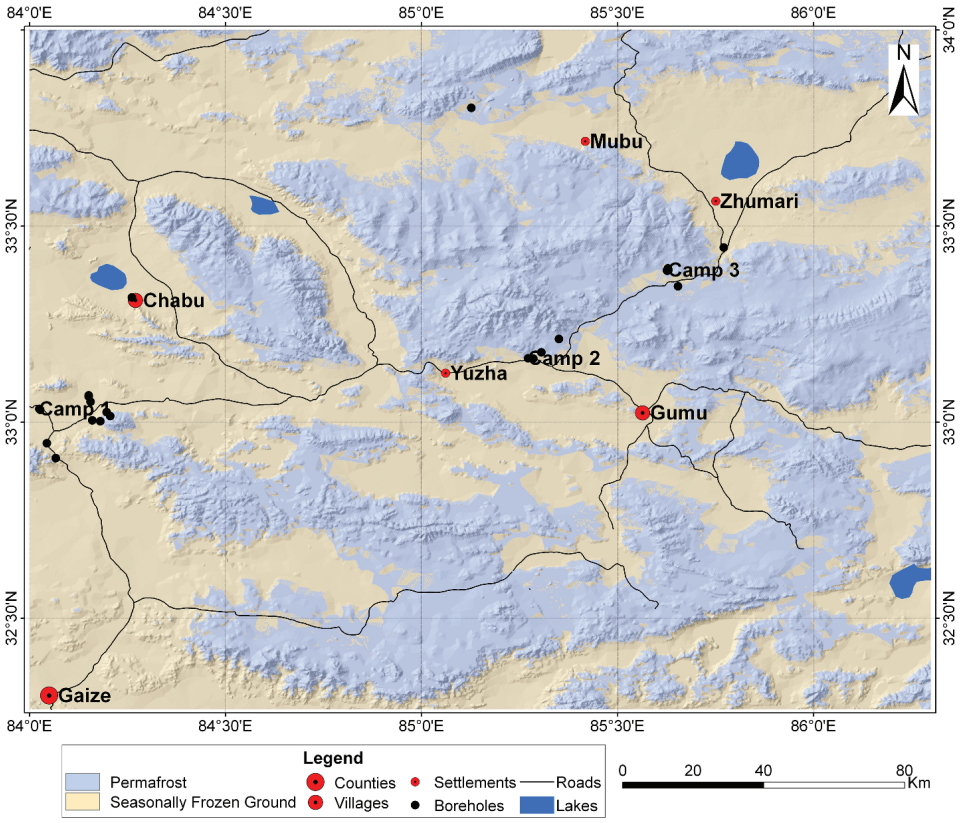

FIGURE 8. Permafrost map of Gaize area based on the current investigation.

in the Gaize area of the western QTP were described and its distribution is simulated. Although the average altitude is >4800 m a.s.l., the discontinuous permafrost is predominant within this region. Temperature measurements and GDP surveys indicate that the MAGT of the widespread alpine steppe is >−1 °C below the altitude of 5400 m a.s.l., permafrost thickness is <60 m, and the active layer is generally deeper than 3 m. Ice-rich permafrost, usually <2 m thick, was found immediately below the active layer. The total ice/water contents of the permafrost are usually <15%. The ALP is closely related to the slope aspect, vegetation community, and physical properties of surface soil horizons. Below the altitude of 4950 m a.s.l., permafrost can be found only on north-facing slopes of marshes. For the alpine steppe, which represents >80% of the total area, the ALP is 5100 m a.s.l. on south-facing slopes, 4950 m a.s.l. on the north-facing slopes, and 5000 m a.s.l. on the east-west–facing slopes. Based on permafrost survey data and a digital elevation model, permafrost distribution in Gaize area was simulated in the ARCGIS platform. The simulated map revealed that the permafrost is distributed mainly in the hilly and mountainous areas, and that it accounts for about 51% of the total investigated area. The large differences between the two maps are mainly due to errors in the mapping method used to create the map of Li and Cheng (1996) and partly due to permafrost degradation.

This paper only provided a primary study regarding permafrost of the Gaize area. Because of the lack of data about salinity and consecutive ground temperature, accuracy of ALT is unsatisfied if it is used to study the degradation of permafrost. Additionally, the investigated area is a small part of the west QTP and hence, applicability of the above conclusions needs further confirmation in the future.

Acknowledgments

This work was financially supported by the National Basic Research Program of China (Grant No. 2013CBA01803), the National Natural Science Foundation of China (Grant No. 41101065), and CAS "Equipment Development Project for Scientific Research" (Grant No. YZ201523). Thanks to the Environmental and Ecological Science Data

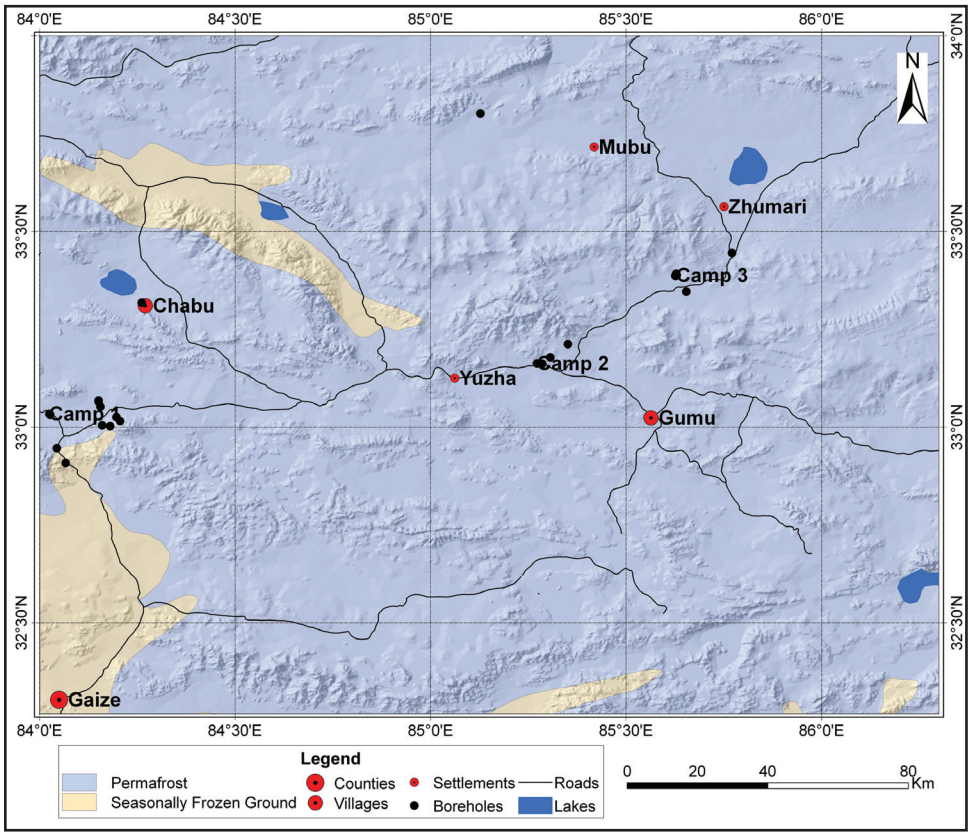

FIGURE 9. Permafrost distribution of Gaize area based on the Permafrost Map of the Qinghai–Tibet Plateau (Li and Cheng, 1996).

Center for West China (http://westdc.westgis.ac.cn/), who provided the 90 m DEM data of the study area, and Editage (http://online.editage.cn/dashboard) for English language editing. We also thank Tingjun Zhang and other two anonymous reviewers for their good advice and every member attending the 2010 permafrost survey in the western Qinghai-Tibet Plateau.

References Cited

Brown, J., Ferrians, O. J., Jr., Heginbottom, J. A., and Melnikov, E. S., 1997: Circum-Arctic map of permafrost and ground ice conditions. Middleton, Wisconsin: Center for Integrated Data Analytics Wisconsin Science Center.

Brown, J., Hinkel, K. M., and Nelson, F. E., 2000: The Circumpolar Active Layer Monitoring (CALM) Program: research design and initial results. *Polar Geography*, 24(3): 165–253, doi http://dx.doi.org/10.1080/10889370009377698.

Cao Xiaobin, Wu Guangning, Fu Longhai, Li Ruifang, and Li Zeng, 2007: Study of the temperature impact on soil resistivity. *Transactions of China Electrotechnical Society*, 22(9): 1–6 (in Chinese).

Cheng Guodong, 1983: Vertical and horizontal zonation of high altitude permafrost. *In* Proceedings, Fourth International Conference on Permafrost. Washington, D.C.: National Academy Press, 136–141.

Cheng Guodong, 1984: Problems on zonation of high-alititude permafrost. *ACTA Geographica SINICA*, 39(2): 185–193 (in Chinese).

Cheng Guodong, and Wu Tonghua, 2007: Responses of permafrost to climate change and their environmental significance, Qinghai-Tibet Plateau. *Journal of Geophysical Research*, 112: F02S03, doi http://dx.doi.org/10.1029/2006JF000631.

CAREERI [Cold and Arid Regions Environmental and Engineering Research Institute, Chinese Academy of Sciences], 2006: Map of the glaciers, frozen ground and desert in China. Beijing: SinoMaps Press (in Chinese), scale 1:4,000,000.

Feng Xuemin, and Cai Deli, 2004: Soil temperature in relation to air temperature, altitude, and latitude. *Acta Pedologica Sinica*, 41(3): 489–491 (in Chinese).

Frauenfeld, O. W., Tingjun, Z., and Barry, R. G., 2004: Interdecadal changes in seasonal freeze and thaw depths in Russia. *Journal of Geophysical Research*, 109: D05101, doi http://dx.doi.org/10.1029/2003JD004245.

French, H. M., 2007: *The Periglacial Environment*. Third edition. Chichester, U.K.: John Wiley & Sons, 480 pp.

He Yixian, 1991: The permafrost investigation with electronic sound method along Xinjiang-Tibetan Highway. *Journal of Glaciology and Geocryology*, 13(3): 255–259 (in Chinese).

Hinkel, K. M., and Nelson F. E., 2003: Spatial and temporal patterns of active layer thickness at Circumpolar Active Layer Monitoring (CALM) sites in northern Alaska, 1975–

2000. *Journal of Geophysical Research*, 108(D2): 8168, doi http://dx.doi.org/10.1029/2001JD000927.

Jin Huijun, Sun Liping, Wang Shaoling, He Ruixia, Lv Lanzhi, and Yu Shaopeng, 2008: Dual influences of local environmental variables on ground temperatures on the Interior-Eastern Qinghai-Tibet Plateau (I):vegetation and snow cover. *Journal of Glaciology and Geocryology*, 30(4): 535–545 (in Chinese).

Lanzhou Institute of Glaciology and Geocryology (LIGG), Chinese Academy of Sciences, 1988: Map of snow, ice and frozen ground in China. Beijing: Cartographic Publishing House (in Chinese), scale 1: 4,000,000.

Li Dongqing, Zhu Linnan, Guo Xingmin, Xing Lili, Fang Jianhong, and Guo Decun, 1998: Brief introduction of Huashixia experiment station of frozen soil roadbed, Qing-Kang Highway. *Scientai Geographica Sinica*, 18(1): 94–95 (in Chinese).

Li Jing, Sheng Yu, Wu Jichun, Chen Ji, and Zhang Xiumin, 2009: Probability distribution of permafrost along a transportation corridor in the northeastern Qinghai Province of China. *Cold Regions Science and Technology*, 59(1): 12–18.

Li Jing, Sheng Yu, Wu Jichun, Wang Jie, Zhang Bo, Ye Baisheng, Zhang Xiumin, and Qin Xiang, 2011: Application of the equivalent-elevation approach to alpine permafrost distribution models in the upper reaches of the Shule River, Qilian Mountains. *Journal of Glaciology and Geocryology*, 34(2): 357–363 (in Chinese).

Li Kun, Chen Ji, Zhao Lin, Zhang Xiumin, Pang Qiangqiang, Fang Hongbing, and Liu Guangyue, 2012: Permafrost distribution in typical area of West Kunlun Mountains derived from a comprehensive survey. *Journal of Glaciology and Geocryology*, 34(2): 447–454 (in Chinese).

Li Shijie, and Li Shude, 1991: Significance and research on the two boreholes of Tianshuihai in the West Kulun Mountains. *Journal of Glaciology and Geocryology,* 13(2):187–188 (in Chinese).

Li Shude, and Cheng Guodong, 1996: Map of permafrost on the Qinghai-Tibet Plateau. Lanzhou: Gansu Culture Press (in Chinese), scale 1:3,000,000.

Li Shude, and Guo Dongxin, 1980: Thermal state and stability of tunnel in Tumengela Coal Mine, Xizang. *Journal of Glaciology and Geocryology,* 2(3): 46–50 (in Chinese).

Li Shude, and He Yixian, 1990: Features of permafrost in the West Kunlun Mountains. *In* Lan Zhou Institute of Glaciology and Geocryology, Chinese Academy of Sciences (eds.), *Proceedings of Fourth National Conference on Glaciology and Geocryology*. Beijing: Science Press, 1–8 (in Chinese).

Li Shude, He Yixian, and Wang Yaqin, 1998: Permafrost and periglacial environments in the Karakorum and Kunlun Mountains. *In* Su zhen, *Glaciers and Environments in the Karakorum and Kunlun Mountains*. Beijing: Science Press, p. 181–215 (in Chinese).

Li Shuxun, Cheng Guodong, and Guo Dongxin, 1996: Numerical simulation on the changes of permafrost on the Qinghai-Tibet Plateau under a persisting warming climate. *Science in China Series D: Earth Sciences,* 26(4): 342–347.

Lin Zhenyao, and Wu Xiangding, 1981: Climatic regionalization of the Qinghai-Xizang Plateau. *ACTA Geographica Sinica*, 36(1): 22–32 (in Chinese).

Lü Lanzhi, Jin Huijun, Wang Shaoling, Xue Xian, He Ruixia, and Yu Shaopeng, 2008: Dual Influences of local environmental variables on ground temperatures on the Interior-Eastern Qinghai-Tibet Plateau (II): sand-layer and surface water bodies. *Journal of Glaciology and Geocryology*, 30(4): 546–555 (in Chinese).

Lu Zijian, Wu Qingbai, Sheng Yu, and Zhang Luxin, 2006: Heat and water difference of active layers beneath different surface conditions near Beiluhe in Qinghai-Xizang Plateau. *Journal of Glaciology and Geocryology*, 28(5): 642–647.

Luo Dongliang, Jin Huijun, Lü Lanzhi, and Wu Qingbai, 2014: Spatiotemporal characteristics of freezing and thawing of the active layer in the source areas of the Yellow River (SAYR). *Chinese Science Bulletin*, 59: doi http://dx.doi.org/10.1007/s11434-014-0189-6.

Ma Wei, Shi Conghui, Wu Qingbai, Zhang Luxin, and Wu Zhijian, 2006: Monitoring study on technology of the cooling roadbed in permafrost region of Qinghai-Tibet plateau. *Cold Regions Science and Technology*, 44(1): 1–11.

Nan Zhuotong, Li Shuxun, and Liu Yongzhi, 2002: Mean annual ground temperature distribution on the Tibetan Plateau: permafrost distribution mapping and further application. *Journal of Glaciology and Geocryology*, 24(2): 142–148 (in Chinese).

Nelson, F. E., Hinkel, K. M., Shiklomanov, N. I., Mueller, G. M., Miller, L. L., and Walker, D. A., 1998: Active-layer thickness in north-central Alaska: systematic sampling, scale and spatial autocorrelation. *Journal of Geophysical Research*, 103D: 28963–28973.

Niu Yun, Liu Xiande, Jing wenmao, Lei Jun, and Che Zongxi, 2013: Comparative study on climate gradient changes in the north slope of Qilian Mountains. *Journal of Gansu Agricultural University*, 48(2): 86–91 (in Chinese).

Pan Baotian, and Li Jijun, 1996: Qinghai-Xizang (Tibetan) Plateau: a driver and amplifier of global climatic changes, III. The effects of the uplift of Qinghai-Tibetan Plateau on climatic changes. *Journal of Lanzhou University (Natural Sciences)*, 32(1): 108–115 (in Chinese).

Pan Baotian, Li Jijun, and Chen Fahu, 1995a: Qinghai-Tibetan Plateau: a driver and amplifier of global climatic changes, I. Basic characteristics of climatic changes in Cenozoic Era. *Journal of Lanzhou University (Natural Sciences)*, 31(3): 120–128 (in Chinese).

Pan Baotian, Li Jijun, and Chen Fahu, 1995b: Qinghai-Xizang (Tibetan) Plateau: a driver and amplifier of global climatic changes, II. Uplift processes of the Qinghai-Xizang (Tibatan) Plateau. *Journal of Lanzhou University (Natural Sciences)*, 31(4): 160–167 (in Chinese).

Pang Qiangqiang, Cheng Guodong, Li Shuxun, and Zhang Wengang, 2009: Active layer thickness calculation over the Qinghai-Tibet Plateau. *Cold Regions Science and Technology*, 57: 23–28.

Qin Dahe, Yao Tandong, Ding Yongjian, and Ren Jiawen, 2014: *Glossary of Cryosphere Science*. Beijing: China Meteorological Press.

Ran Youhua, Li Xin, Cheng Guodong, Zhang Tingjun, Wu Qingbai, Jin Huijun, and Jin Rui, 2012: Distribution of permafrost in China: an overview of existing permafrost maps. *Permafrost and Periglacial Processes*, 23(4): 322–333.

Sheng Yu, Fang Jianhong, Zhang Xiumin, Huang Shijing, and Cao Yuanbing, 2012: Distribution pattern and mapping of

permafrost along the National Highway No.214. *In* Ma Wei and Niu Fu Jun, *Research Monograph of Cold and Arid Regions Engineering and Environment*. Lanzhou: Lanzhou University Press, 221–228 (in Chinese).

Sun Honglie, 1996: *Formation and Evolution of Qinghai-Tibet Plateau*. Shanghai: Press of Science and Technology, 1-9 (in Chinese).

Tan Chunping, Yang Jianping, and Mi Rui, 2010: Analysis of the climate change characteristics in the Southern Tibetan Plateau from 1971 to 2007. *Journal of Glaciology and Geocryology*, 32(6): 1111–1120 (in Chinese).

Tong Boliang, Li Shude, Pu Jianchen, and Qiu Guoqing, 1983: Principle and method of compilation of map of the distribution of permafrost along the Qinghai-Tibetan Highway (1:600,000). *In* Lanzhou Institute of Glaciology and Geocryology, Chinese Academy of Sciences (eds.), *Proceedings of the 2nd Chinese Conference on Glaciology and Geocryology*. Lanzhou: Gansu People's Press, 52–57 (in Chinese).

Wang Jun, Huang Shangyao, Huang Geshan, and Wang Jishang, 1990: *Geothermic Characteristics in China*. Beijing: Publishing House of Earthquake, 10–98 (in Chinese).

Wang Shaoling, 1997: Study of permafrost degradation in the Qinghai-Xizang Plateau. *Advances in Earth Sciences*, 12(2): 164–167 (in Chinese).

Wang Shaoling, Luo Xiangrui, and Guo Pengfei, 1991: The distributive characteristics of frozen ground in the east of Qinghai-Xizang Plateau. *Journal of Glaciology and Geocryology*, 13(2): 131–140 (in Chinese).

Wang Shaoling, Zhao Xiufeng, Guo Dongxin, and Huang Yizhi, 1996: Response of permafrost to climate change in the Qinghai-Xizang Plateau. *Journal of Glaciology and Geocryology*, 18 (special): 157–165 (in Chinese).

Wang Shaoling, Lin Qing, and Zhao Lin, 1999: Permafrost along the Qing-Kang Highway (National Highway No. 214). *Arid Land Geography*, 22(2): 42–49 (in Chinese).

Wang Shaoling, Jin Huijun, Li Shuxun, and Zhao Lin, 2000: Permafrost degradation on the Qinghai-Tibet Plateau and its environmental impacts. *Permafrost and Periglacial Processes*, 11: 43–53.

Washburn, A. L., 1979: *Geocryology: A Survey of Periglacial Processes and Environments*. London: Edward Arnold.

Wei Chunling, Wu Shengzhi, Li Dongqing, and Fang Jianhong, 1999: Relationship between climate changes and permafrost degradation at Huashixia Valley, China. *Journal of Lanzhou University (Natural Sciences)*, 35(1): 206–210.

Wu Jichun, Sheng Yu, Yu Hui, and Li Jinping, 2007a: Permafrost characteristics in the central-east Qilian Mountains (I): permafrost distribution. *Journal of Glaciology and Geocryology*, 29(3): 418–425 (in Chinese).

Wu Jichun, Shengyu, Yu Hui, and Li Jinping, 2007b: Permafrost characteristics in the central-east Qilian Mountains (II): permafrost distribution. *Journal of Glaciology and Geocryology*, 29(3): 426–432 (in Chinese).

Wu Jichun, Shengyu, Li Jing, and Wang Jie, 2009: Permafrost in the source of Shule River. *Acta Geographica Sinica*, 64(5): 571–580 (in Chinese).

Wu Qingbai, and Zhang Tingjun, 2008: Recent permafrost warming on the Qinghai-Tibetan Plateau. *Journal of Geophysical Research*, 113: D13108, doi http://dx.doi.org/10.1029/2007JD009539.

Wu Qingbai, and Zhang Tingjun, 2010: Changes in active layer thickness over the Qinghai-Tibetan Plateau from 1995 to 2007. *Journal of Geophysical Research*, 115: D09107, doi http://dx.doi.org/10.1029/2009JD012974.

Wu Qingbai, Lu Zijian, and Liu Yongzhi, 2005: Permafrost monitoring and its recent changes in Qinghai-Tibet Plateau. *Advances in Climate Change Research*, 1(1): 26–28 (in Chinese).

Wu Qinghai, Zhang Tingjun, and Liu Yongzhi, 2012: Thermal state of the active layer and permafrost along the Qinghai-Xizang (Tibet) Railway from 2006 to 2010. *The Cryosphere*, 6: 607–612, doi http://dx.doi.org/10.5194/tc-6-607-2012

Wu Tonghua, Li Shuxun, Cheng Guodong, and Nan Zhuotong, 2005: Using ground-penetrating radar to detect permafrost degradation in the northern limit of permafrost on the Tibetan Plateau. *Cold Regions Science and Technology*, 41: 211–219, doi http://dx.doi.org/10.1016/j.coldregions.2004.10.006.

Yu Qihao, K. Roth, Jin Huijun, Pan Xicai, P. M. Schiwek, Sheng Yu, Wei Zhi, and Wu Jichun, 2006: Progress of the Sino-German Joint Researches on the Degradation of Permafrost on the Tibetan Plateau. *Journal of Glaciology and Geocryology*, 28(6): 84–89 (in Chinese).

Zeng Qunzhu, Li Shude, Wang Shaoling, Liang Fengxian, Zhang Yimin, Ye Shiqiang, and Pan Baimin, 1996: Some permafrost environment problems with respect to the western channel project of the south-north water diversion in the region of the Tongtian-Yalong Rivers, China. *Journal of Glaciology and Geocryology*, 18(3): 201–209 (in Chinese).

Zhang, Tingjun, Frauenfeld, O.W., Serreze, M. C., Etringer, A., Oelke, C., McCreight, J., Barry, R. G., Gilichinsky, D., Yang, D., Ye, H., Ling, F., and Chudinova, S., 2005: Spatial and temporal variability in active layer thickness over the Russian Arctic drainage basin. *Journal of Geophysical Research*, 110: D16101, doi http://dx.doi.org/10.1029/2004JD005642.

Zhao Lin, Guo Dongxin, and Li Shuxun, 1998: The past and future of the observation and research station of the Qinghai-Tibet Plateau. *Journal of Glaciology and Geocryology*, 20(3): 287–292 (in Chinese).

Zhao Lin, Wu Qingbai, Marchenko, S. S., and Sharkhuu, N., 2010: Thermal state of permafrost and active layer in central Asia during the International Polar Year. *Permafrost and Periglacial Processes*, 21(2): 198–207.

Zhou Youwu, 1965: Permafrost along the Qinghai-Tibet Highway. *In* Lan Zhou Institute of Glaciology and Geocryology, Chinese Academy of Sciences (eds.), *Proceedings of Permafrost Survey on the Qinghai-Tibet Highway*. Beijing: Science Press, 1–10 (in Chinese).

Zhou Youwu, and Du Rongheng, 1963: Primary investigation on the permafrost of Qinghai-Tibetan Plateau. *Chinese Science Bulletin*, 2: 60–63 (in Chinese).

Zhou Youwu, QiuGuoqing, GuoDongxin, Cheng Guodong, and Li Shude, 2000: *Permafrost in China*. Beijing: Science Press (in Chinese).

MS submitted 26 February 2014
MS accepted 14 March 2016